THRUSTER LIMITATION CONSIDERATION FOR FORMATION FLIGHT CONTROL

Yunjun Xu,
PH.D. Candidate
Department of Aerospace and Mechanical Engineering
University of Florida
Gainesville, FL, 32611

Dr. Norman Fitz-Coy
Associate Professor
Department of Aerospace and Mechanical Engineering
University of Florida
Gainesville, FL, 32611

Dr. Paul Mason
Mission Engineering and Systems Analysis Division
Flight Dynamics Analysis Branch
Goddard Space Flight Center
Greenbelt, Maryland 20771

ABSTRACT

Physical constraints of any real system can have a drastic effect on its performance. Some of the more recognized constraints are actuator and sensor saturation and bandwidth, power consumption, sampling rate (sensor and control-loop) and computation limits. These constraints can degrade system's performance, such as settling time, overshoot, rising time, and stability margins. In order to address these issues, researchers have investigated the use of robust and nonlinear controllers that can incorporate uncertainty and constraints into a controller design. For instance, uncertainties can be addressed in the synthesis model used in such algorithms as H_∞ or μ. There is a significant amount of literature addressing this type of problem. However, there is one constraint that has not often been considered; that is, actuator authority resolution. In this work, thruster resolution and controller schemes to compensate for this effect are investigated for position and attitude control of a Low Earth Orbit formation flight system.

In many academic problems, actuators are assumed to have infinite resolution. In real system applications, such as formation flight systems, the system actuators will not have infinite resolution. High-precision formation flying requires the relative position and the relative attitude to be controlled on the order of millimeters and arc-seconds, respectively. Therefore, the minimum force resolution is a significant concern in this application. Without the sufficient actuator resolution, the system may be unable to attain the required pointing and position precision control. Furthermore, fuel may be wasted due to high-frequency chattering phenomena when attempting to provide a fine control with inadequate actuators.

To address this issue, a Sliding Mode Controller is developed along with the boundary Layer Control to provide the best control resolution constraints. A Genetic algorithm is used to optimize the controller parameters according to the states error and fuel consumption criterion. The tradeoffs and effects of the minimum force limitation on performance are studied and compared to the case without the limitation. Furthermore, two methods are proposed to reduce chattering and improve precision.

I. INTRODUCTION

Physical constraints can be enforced in hardware or software. Software limitations ensure the life of the system by reducing wear and tear on the actuators. For example, a very large step size or impulse control command might damage the equipment, and the saturation of the actuator may degrade the system performance and stability [8]. The effects and control of other hard nonlinearities, such as saturation and bandwidth limits have been investigated by numerous researchers. For instance, References 5-7 discuss how limitation on the maximum force and slew rate can be incorporated into the synthesis model of a H_∞ or μ controller. Nonlinear controllers such as sliding mode can also be used successfully with actuator and slew rate saturations as discussed in Refs. 2-4. In sliding mode control, the saturation is addressed by the control command saturation and the sliding surface together. The slew rate is accounted for by the controller's parameter.

A physical constraint that is not routinely considered is actuator resolution and its effect on the performance. In low-precision applications, actuator resolution is not a concern since the desired precision may be orders of magnitude above the actuator capability. In a high-precision formation flight application, thruster resolution (minimum thrust impulse) must be addressed. Lack of actuator resolution can lead to performance degradation, such as high frequency chattering. For example, controller designs based on the sliding mode concept are susceptible to high frequency chattering unless an integrated boundary layer function is implemented. For cases in which the thruster has a minimum force limitation, high frequency chattering may still exist even with the boundary layer integrated into the sliding mode controller design. This is also addressed in this paper.

Section II lists the symbols, abbreviations and acronyms used in this paper. Section III discusses the dynamics model, the control strategy, and the optimization method on which the actuator limitation effect and proposed control methods are based. This work is implemented in simulation on a Low Earth Orbit formation mission. Section IV discusses the effects of the thruster limitation in terms of predefined performance criteria, fuel consumption, control precision and chattering phenomenon. Sections V and VI present two methods that were studied in order to mitigate chattering and improve control precision in the presence of the thrust resolution issue. Section VII provides conclusions and discussions for future work.

II. SYMBOLS, ABBREVIATIONS AND ACRONYMS

$\overset{\circ}{()}$: the time derivative with respect to a localized frame

$()'$: the true anomaly derivative

$\| \|$: norm 2

$| |$: absolute value

mN: milliNewton

LEO: Low Earth Orbit

BLC: boundary layer control

$diag$: diagonal matrix

GA: genetic algorithm

SMC: sliding mode control

f : true anomaly

$\underline{\underline{J}}$: inertia matrix of the satellite

$\underrightarrow{\rho}$: relative position vector

$\underrightarrow{R}$: absolute position vector

R : magnitude of the absolute position

$\underline{u}$: normalized force w.r.t. the mass

μ : gravitational coefficient

$x^{(j)}$: j^{th} derivative of x

LVLH: local vertical local horizontal coordinate frame

Subscript F or L: follower or leader satellite

Subscript p: position

Superscript L: expressed in the leader's local frame

III. DYNAMICS, CONTROL, OPTIMIZATION[2, 3, 4], AND SIMULATION CONDITION

Dynamics Model

This paper adopts the generalized coupled dynamics model[2, 3, 4] for the leader-follower satellites pair in the formation flight system as the basic model. Eq. (1.1) shows the generalized relative position model expressed in LVLH and can be used in both the circular and elliptic reference orbit.

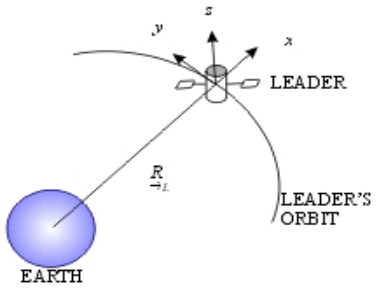

Figure 1 LVLH Coordinate of the Leader's Frame

$$ {}^{L}\underrightarrow{\rho}'' = \frac{1}{\overset{\circ}{f}_L^{\,2}}\{-{}^{L}\underrightarrow{\rho}'\overset{\circ\circ}{f}_L - {}^{L}\overset{\circ}{\underline{\omega}}_L \times {}^{L}\underrightarrow{\rho} - 2\,{}^{L}\underline{\omega}_L \times {}^{L}\underrightarrow{\rho}'\overset{\circ}{f}_L - {}^{L}\underline{\omega}_L \times ({}^{L}\underline{\omega}_L \times {}^{L}\underrightarrow{\rho}) + \frac{\mu}{R_L^3}[\underline{R}_L - (\frac{R_L}{R_F})^3\underline{R}_F] + (\underline{u}_F - \underline{u}_L)\} \tag{1.1} $$

The detailed information of the dynamics can be found in Ref [2] and is not presented in this paper.

Sliding Mode Controller

If $\underline{x} = [\rho_1, \rho_2, \rho_3]^T$ is the system state, then the dynamics model of the leader-follower pair can be expressed as

$$ \underline{x}^{(n_i)} = \underline{f}(\underline{x}, \underline{x}^{(1)}, ..., \underline{x}^{(n_i-1)}) + \underline{\underline{B}}(\underline{x}, \underline{x}^{(1)}, ..., \underline{x}^{(n_i-1)})\underline{u} \tag{1.2} $$

where $\underline{\underline{B}} = \left[b_{ij}\right]_{m\times m}$ is the input influence matrix and $\underline{f} = [f_i]_{m\times 1}$ describes the dynamics of the system. The sliding surface is defined as

$$ s_i = (\frac{d}{dt} + \lambda_i)^{(n_i-1)}\tilde{x}_i = x_i^{(n_i-1)} - x_{ri}^{(n_i-1)} \tag{1.3} $$

Here $\underset{\sim}{\tilde{x}} = \underset{\sim}{x} - \underset{\sim}{x}_{DESIRED}$ is the tracking error, and $x_{ri}^{(n_i-1)} = x_{DESIRED}^{(n_i-1)} - \lambda_i^{n_i-1}\tilde{x}_i$. Then the SMC is given by Eq. (1.4), in which, $\underset{\sim}{x}_r^{(n-1)} = \left[x_{r1}^{(n_1-1)} \quad x_{r2}^{(n_2-1)} \quad \cdots \quad x_{rm}^{(n_m-1)} \right]^T$ and $\underset{\rightarrow}{k}\,\mathrm{sgn}(\underset{\rightarrow}{s}) = [k_i\,\mathrm{sgn}(s_i)]_{m\times 1}$. k is defined as the sum of the uncertainty in the model plus η. If the model is assumed to be exact, then $k_i = \eta_i$. Based on the stability analysis from the literature, $\lambda_i > 0$ and $\eta_i > 0$[9]. In sliding mode control, parameter k_i affects $\tilde{x}$ and $\dot{\tilde{x}}$, whereas, λ_i affects $\tilde{x}$.

$$\underset{\sim}{\hat{u}} = \underset{\equiv}{B}^{-1}[\underset{\sim}{x}_r^{(n-1)} - \underset{\rightarrow}{f} - \underset{\rightarrow}{k}\,\mathrm{sgn}(\underset{\rightarrow}{s})] \tag{1.4}$$

In order to mitigate the chatter, the boundary layer control (BLC) concept is introduced as in Refs. [1, 3, 4]. In the BLC, the sliding surface includes a hard switching outside of the boundary, and a soft switching inside of the boundary. With the addition of BLC, the performance of the controller is smoother and more efficient. Equation (1.5) is used to replace the sign function in Eq. (1.4), where ε_i is a nonzero positive value. When ε_i goes to infinity, the switching becomes the hard switching. Smaller ε_i produce a smoother but slower response.

$$sign(s_i) \Rightarrow sat(\frac{s_i}{\varepsilon_i}) = \begin{cases} \mathrm{sgn}(s_i) & s_i \geq 1 \\ \dfrac{s_i}{\varepsilon_i} & s_i < 1 \end{cases} \qquad i = 1,2,...m \tag{1.5}$$

Parametric Optimization

Nine parameters are used to design the SMC-BLC controller for the relative position model (Eq. (1.6)). For a system that is highly nonlinear and has a long evaluation time, the conventional large-scale optimization does not work well. Therefore, a genetic algorithm search approach is utilized in order to expedite the selection of the parameters and also to obtain an "optimized" set of parameters. The population size and number of generation are all twenty. The bit length is forty, and the crossover and mutation probabilities are 0.9 and 0.05 separately. In order to reduce the calculation time, thruster working frequency is chosen as 0.5 Hz, and each evaluation time equals the period of the leader's orbit. Since the full parameter space is not considered, there are no claims of global optimality.

$$\begin{aligned} &\text{In SMC: } \underset{\rightarrow}{k}_p \in R^{3\times 1} \quad \underset{\rightarrow}{\lambda}_p \in R^{3\times 1} \\ &\text{In BLC: } \underset{\rightarrow}{\varepsilon}_p \in R^{3\times 1} \end{aligned} \tag{1.6}$$

IV. EFFECTS OF THRUSTER LIMITATIONS

Simulation Condition

The LEO formation system considered has both the leader and follower in 500 km altitude circular orbits. The leader's orbit is equatorial and the follower's orbit has an inclination of 0.1^0. At simulation epoch, the leader's true longitude is 0^0 and the follower is -0.1^0. The small angular difference ensures the relative position of the formation system is on the order of 10 km and that the relative angles are small enough for small angle approximation. It is assumed that the simulated system has a thruster configuration that provides uncoupled thrust and torques in all directions. The objectives are maintaining the satellites in the fixed formation and not exceeding the physical limitation. The design requirements are to produce a stable system and find a balance between control precision, chatter, and fuel consumption. In future works, specific requirements such as jitter, controller bandwidth, attitude and position accuracy, and slew requirements will be used. From Section IV through Section VI, the relative position performance will be used to show the effects of the thruster limitation, and comparison of the two proposed chatter mitigation methods.

Thruster without Limitation

In order to generalize this work, the command and thruster forces are normalized with respect to the mass of the spacecraft. This also allows for force equivalence between different size spacecrafts in the formation. In the first the case, which does not use the maximum and minimum limits, control parameters $\underset{\rightarrow}{k} = [100,100,520]^T$, $\underset{\rightarrow}{\lambda} = [0.1,0.1,0.1]^T$, $\underset{\rightarrow}{\varepsilon} = [0.01,0.01,0.01]^T$ are chosen by trial and error. Figure 2 and Figure 3 illustrate the force commands where maximum and minimum thruster limitations do not exist. Because x and y directions are in plane and z is out of

plane, the initial velocity and force command in the z direction is much larger than that in the x and y directions. The saturation level in the z direction is due to the saturation in the sliding surface instead of the saturation in the thruster.

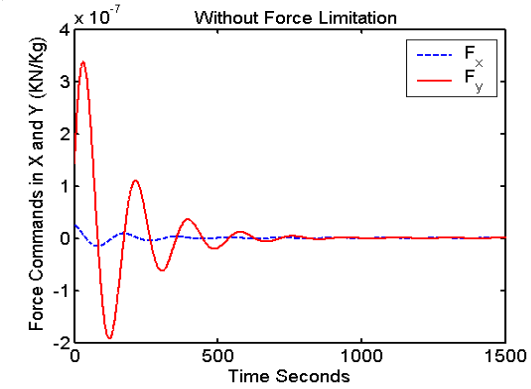

Figure 2 Normalized force commands in X and Y directions of LVLH

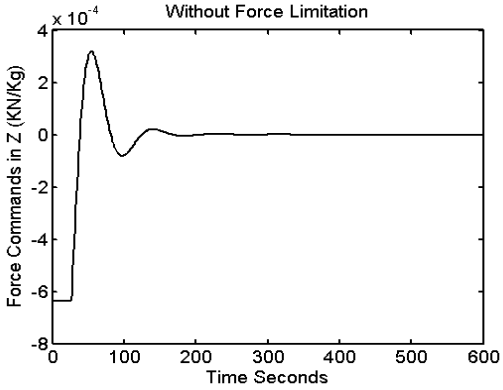

Figure 3 Normalized force commands in Z direction of LVLH

Thruster with Maximum Limitation

The thruster configuration is assumed to provide different maximum forces in each direction [1 mN 2 mN 2 N] in xyz respectively. Figures 4 through 6 display the simulation results when the thruster has the maximum limitations. If thruster doesn't have a minimum thrust limitation, the resulting relative position error is on the order of micrometer. Figure 7 provides the results of the relative position error in z direction when no maximum limitation is enforced. A comparison of Figure 5 and Figure 7 illustrates that the saturation in the thruster induces a longer transient stage, more oscillations, and larger overshoot.

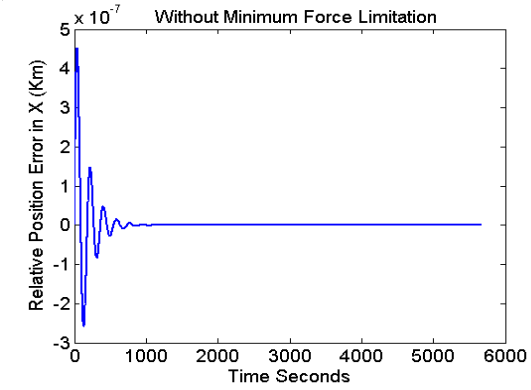

Figure 4 Relative position in x of LVLH with maximum force limitation

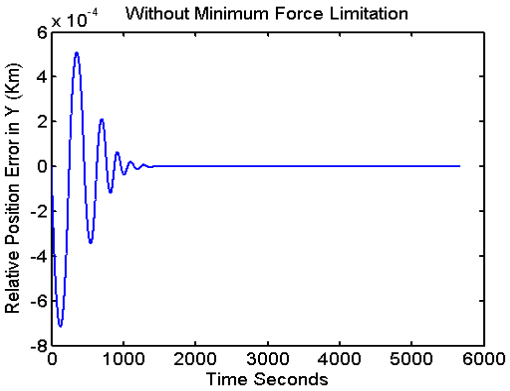

Figure 5 Relative position in y of LVLH with maximum force limitation

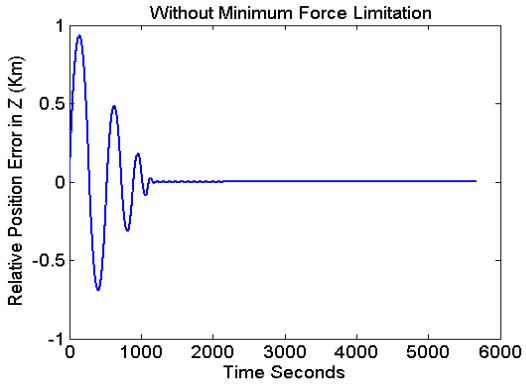

Figure 6 Relative position in z of LVLH with maximum force limitation

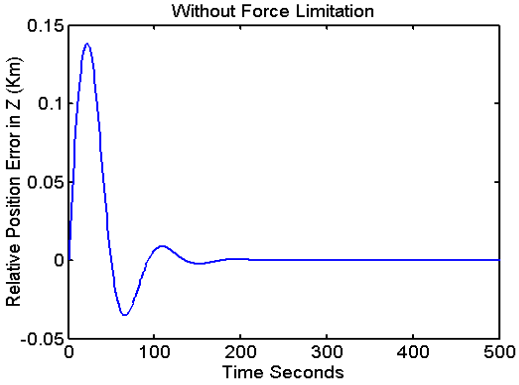

Figure 7 Relative position in z of LVLH without force limitation

Thruster with Maximum and Minimum Limitation

Simulations are conducted and compared for different maximum and minimum force ratios. The maximum force ratio is with respect to *F_s*=[1mN 2mN 2N]. For example, a maximum force ratio of two corresponds to 2**F_s* means the maximum force is 2*[1mN 2mN 2N]. The minimum ratio is with respect to the maximum force so 2% means that the minimum force the thruster can provide is 2% of the maximum force. The performance criterion is calculated by $J = \int_0^{t_f} \left\| \underline{x}(t) - \underline{x}_{des}(t) \right\| dt$, where $\underline{x}_{Des}$ represents the desired state vector. The limitations constraints is defined as

$$u = \begin{cases} 0 & if \ |u| <= u_{\min} \\ sign(u)u_{\max} & if \ |u| >= u_{\max} \\ u & other \end{cases} \tag{1.7}$$

Table 1 demonstrates that the minimum thrust ratio does not significantly affect the performance because the performance criterion is dominated by the transient stage and the control precision is in the stable stage. Instead, the performance criterion is reduced as the maximum thruster force increases. The increase in thrust levels reduces the settling time.

The fuel consumption of the different cases is compared Table 2. For the relative position and velocity, error is linearly correlated with the control effort in SMC + BLC, therefore, the trend in Table 2 is similar to that of Table 1. Considering the maximum force level, performance criterion, and fuel consumption in both tables, the maximum ratio of 4 is chosen as the base line thruster in later simulations. Therefore, the maximum forces the thruster can provide in three directions are [4 8 8000] milliNewton.

Table 1 Performance Criterion Comparison for Different Maximum and Minimum Level

Min Ratio → / Max Ratio ↓	0%	2%	4%	6%	8%	10%
1	15.1416	15.1416	15.1417	15.1421	15.1426	15.1405
2	4.4977	4.4979	4.4988	4.4994	4.5005	4.5012
4	1.4726	1.4749	1.4812	1.4900	1.5005	1.5109
6	0.8161	0.8250	0.8459	0.8735	0.8900	0.9221
8	0.6872	0.7043	0.7381	0.7947	0.8479	0.8194
10	0.6872	0.7128	0.7689	0.8226	0.8194	0.9820

Table 2 Fuel Consumption in sum sense $J = \int_0^{t_f} (\sum_{i=x,y,z} |u_i|) dt$

Min Ratio → / Max Ratio ↓	0%	2%	4%	6%	8%	10%
1	0.1083	0.1082	0.1081	0.1081	0.1081	0.1079
2	0.0622	0.0620	0.0619	0.0618	0.0617	0.0616
4	0.0397	0.0395	0.0393	0.0391	0.0389	0.0388
6	0.0335	0.0332	0.0329	0.0327	0.0324	0.0321
8	0.0316	0.0312	0.0308	0.0304	0.0300	0.0296
10	0.0316	0.0310	0.0304	0.0300	0.0296	0.0292

Based on the tables above, if the limitation constraint technique is used for the same thruster, then the performance criterion and fuel consumption do not change significantly. In Figures 8 - 15, the time responses of the relative position error and control efforts are shown. The precision of the relative position is increased with the thruster resolution capabilities (i.e., better precision is obtained with the 0% case), as seen in Figures 8 – 11. In the z direction, the control precisions are on the order of $O(10^{-11})$, $O(10^{-3})$, and $O(10^{-3})$ km, respectively for the 0%, 4%, and 10% cases. It should also be noted that higher control precision is achieved at the expense of significant chattering.

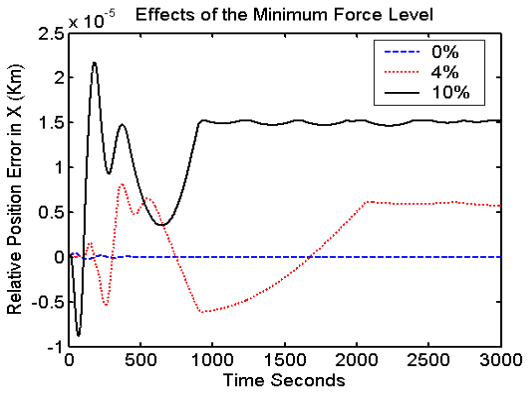

Figure 8 Relative position error in x of LVLH for different min force level

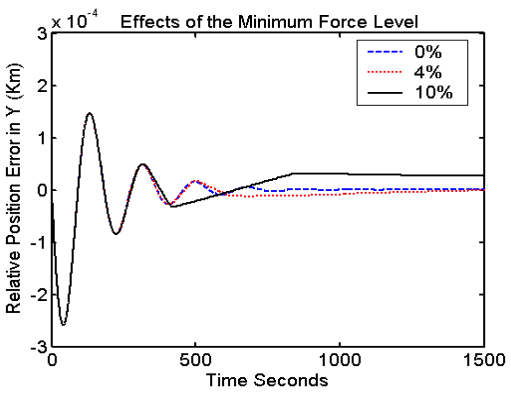

Figure 9 Relative position error in y of LVLH for different min force level

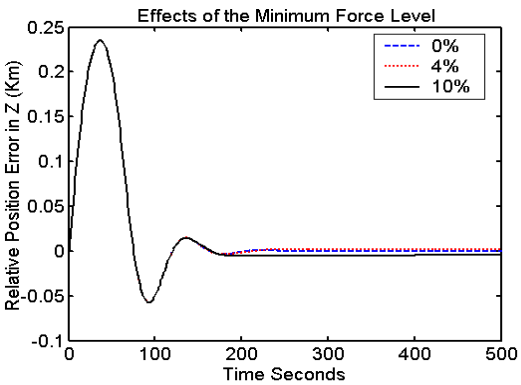

Figure 10 Relative position error in z of LVLH for different min force level

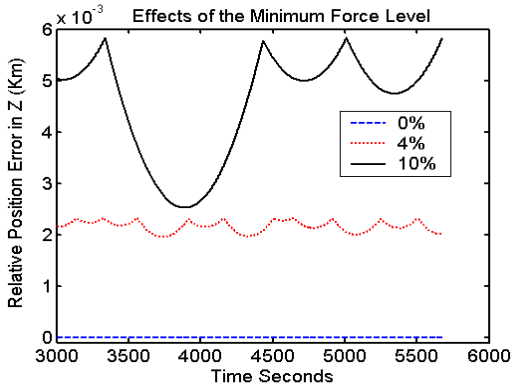

Figure 11 Relative position error in z of LVLH for different min force level from 3000 to 6000 seconds

Figures 12 - 15 illustrate the time response of the thruster forces. The 0% (infinite resolution) thruster case is smooth and has no chattering, whereas the 10% case gives more chatter. Figure 15 contains the time response for the 10% case, which has several spikes due to the resolution. In each Figure there are 3 minimum force percentages. The higher the percentage, the more likely chatter will occur.

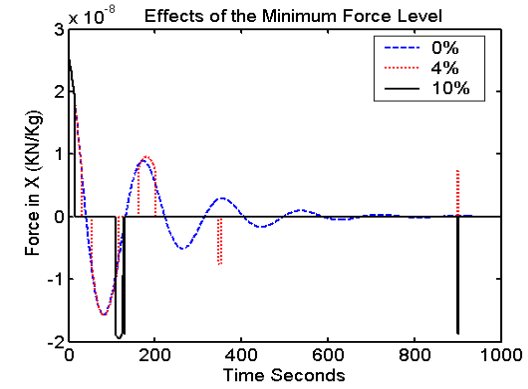

Figure 12 Normalized thruster force in x of LVLH

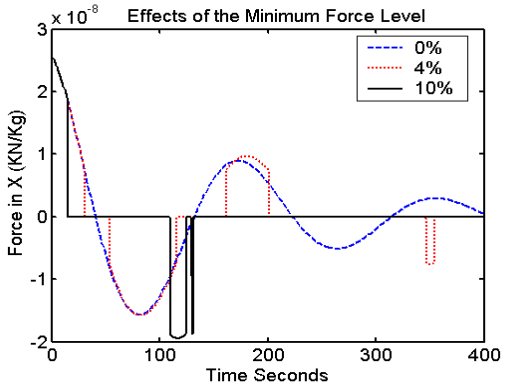

Figure 13 Normalized thruster force in x of LVLH from 0- 400 seconds

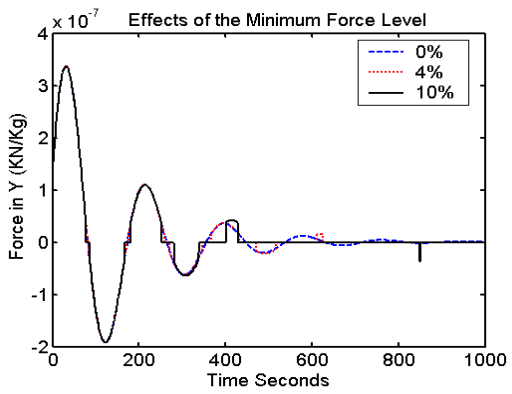

Figure 14 Normalized thruster force in y of LVLH

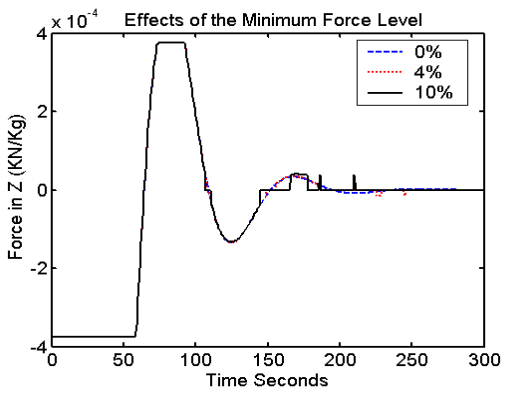

Figure 15 Normalized thruster force in z of LVLH

V. COMPARISON OF DIFFERENT PREFILTERS

As seen in the results from the previous section, the chattering and lowest achievable relative position error are associated with the discontinuity of the thruster force commands. In this section, we discuss a pre-filter concept to mitigate this discontinuity generated by the SMC. The idea is to attempt to map the control commands generated by the SMC to "smooth" thrust commands. A total of three pre-filters are compared. Pre-filter 1 is the baseline case used normally and is described in Eq. (1.8); pre-filters 2 and 3 are described in Eqs. (1.9) and (1.10), respectively. Figure 16 provides a graphical description of all three pre-filters. It can be observed that pre-filters 2 and 3 have 3 discontinuities and pre-filter 1 has 4 discontinuities. Both pre-filters 2 and 3 try to balance the total forces by increasing the force below the minimum, and decreasing the force above the minimum.

Pre-filter 1 (cut off case):

$$u = \begin{cases} 0 & if\ |u| <= u_{\min} \\ sign(u)u_{\max} & if\ |u| >= u_{\max} \\ u & other \end{cases} \tag{1.8}$$

Pre-filter 2:

$$u = \begin{cases} u_{\min} & if\ u = 0 \\ sign(u)[u_{\min} + \dfrac{|u|}{u_{\max} \times ratio}(u_{\max} - u_{\min})] & if\ u \neq 0\ |u| <= u_{\max} \\ sign(u)u_{\max} & if\ |u| > u_{\max} \end{cases} \tag{1.9}$$

Pre-filter 3:

$$u = \begin{cases} u_{\min} & if\ u = 0 \\ sign(u)[\dfrac{u_{\max} - u_{\min}}{u_{\max}^{2}}u^{2} + u_{\min}] & if\ u \neq 0 and\ |u| <= u_{\max} \\ sign(u)u_{\max} & if\ |u| > u_{\max} \end{cases} \tag{1.10}$$

Figures 17 - 22 present the relative position error and resultant force for the three pre-filters. Although the pre-filter 1 has a larger stable-state error, which is on the order of centimeter level, it results in very low chattering. In Table 3, for the fuel consumption case, pre-filter 1 also yielded the lowest fuel consumption, whereas, the other performance criteria for all three cases were similar. Pre-filters 2 and 3 both generate the force above the required one, therefore, chattering is more severe than the pre-filter 1.

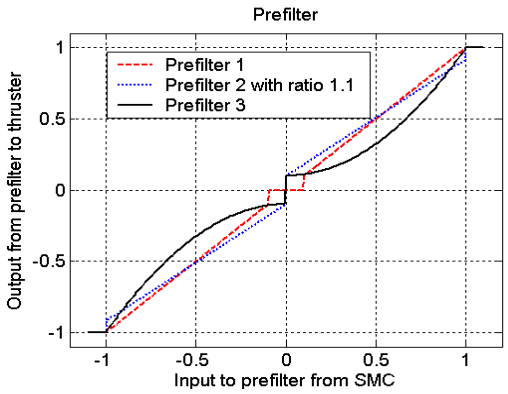

Figure 16 Three pre-filters

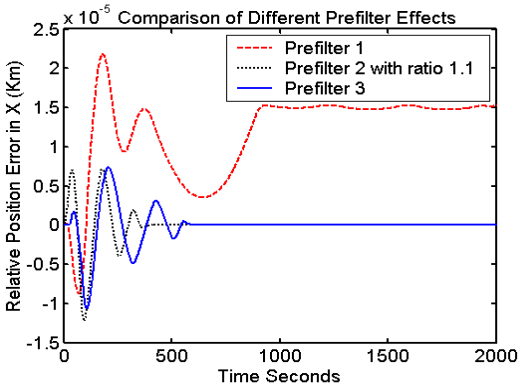

Figure 17 Relative position in X of LVLH

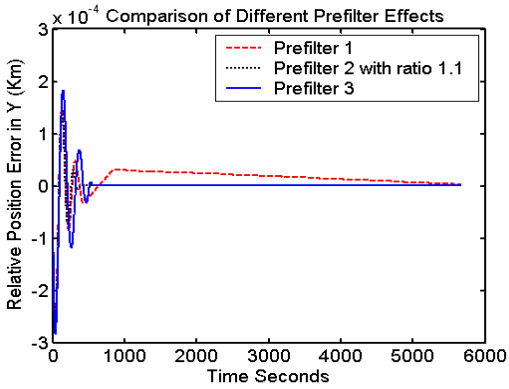

Figure 18 Relative position in Y of LVLH

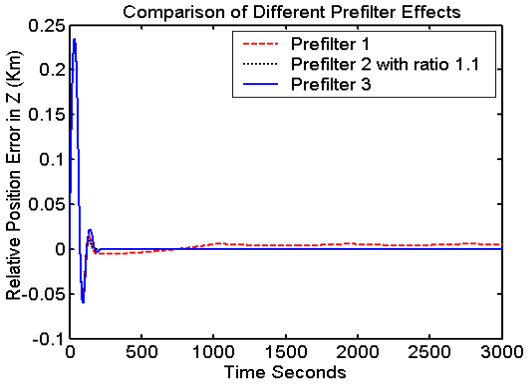

Figure 19 Relative position in Z of LVLH

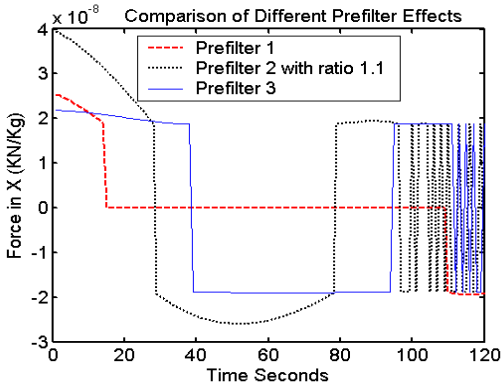

Figure 20 Normalized force in X of LVLH

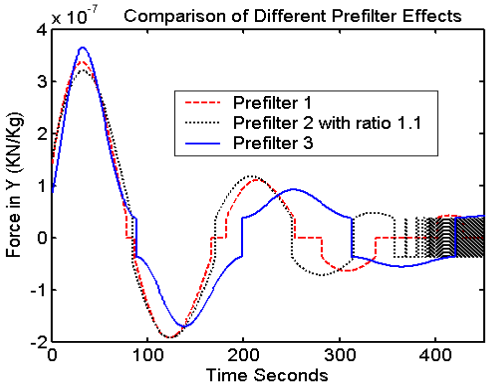

Figure 21 Normalized force in Y of LVLH

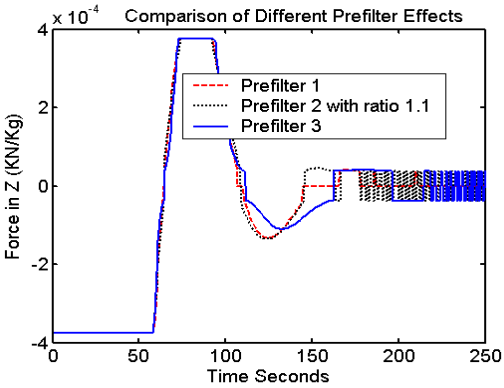

Figure 22 Normalized force in Z of LVLH

Table 3 Performance and Fuel Consumption Comparison for Different Pre-filters

	Performance Criterion	Fuel Consumption in Sum Sense
Pre filter 1	1.5109	0.0388
Pre filter 2	1.4730	0.2473
Pre filter 3	1.4800	0.2456

VI. COMPARISON OF DIFFERENT BLC

The boundary layer function is modified in order to mitigate the chattering. In Figure 23, three boundary layer functions are introduced which have 2, 5, and 3 discontinuities respectively.

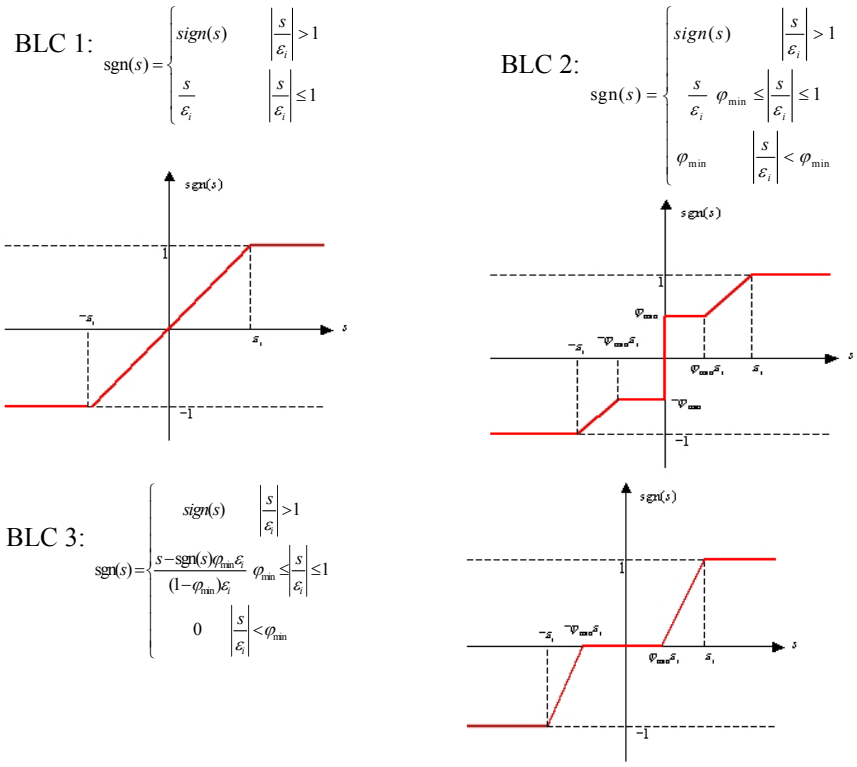

Figure 23 Three different BLCs

Table 4 shows the comparisons of the different boundary layer control schemes based on cost, fuel consumption, control precision and chattering. Here, the chatter is defined as the number of jumps in the control effort during simulation time period from 4000 to 6000 seconds in all directions. Cases 3 and 5 use the GA to determine the optimal $\varphi_{\min}$. The cost is calculated by $J = \frac{1}{2}\int [\underline{e}^T \underline{\underline{Q}} \underline{e} + \underline{u} \underline{\underline{R}} \underline{u}] dt$. In order to generate relatively equal contributions from all three directions in the cost, the weights are chosen to be $\underline{\underline{Q}} = diag[2000,1000,1]$ and $\underline{\underline{R}} = diag[1000,100,1]$ since the z-direction's relative position error and control efforts are very different from those of the x- and y-directions. Fuel consumptions for all the cases are on the same order. However, without GA, the BLC 2 and BLC 3 cases yield high cost functions and low precisions. The last column in Table 4 provides a qualifier of the chatter from 4000 to 6000 seconds of the simulation for three directions.

It is worth noting that when the parameters for BLC 2 and BLC 3 are obtained from the GA, both cases converge to BLC 1 and the optimal results are the same as that of BLC 1. Therefore, it can be concluded that BLC 1 provides the best solution among all three BLC designs. The time responses of the relative position error and control efforts are the same as the pre-filter 1 case shown in Figures 17 - 22.

Table 4 Comparison of different BLC

	φ_{min}	Cost	Fuel	Control Precision in Km	Chattering / 4000~6000 sec
BLC 1	0	1.1423	0.0388	$[10^{-5}; 10^{-5}; 10^{-3}]$	[2; 0; 0]
BLC 2	0.2	423.4600	0.0370	$[10^{-2}; 10^{-2}; 10^{-2}]$	[1; 8; 0]
BLC 2 & GA	1.22e-5	1.1423	0.0388	$[10^{-5}; 10^{-5}; 10^{-3}]$	[0; 0; 0]
BLC 3	0.2	371.5605	0.0367	$[10^{-2}; 10^{-2}; 10^{-2}]$	[1; 7; 0]
BLC 3 & GA	6.65e-5	1.1398	0.0387	$[10^{-5}; 10^{-5}; 10^{-3}]$	[1; 2; 0]

VII. CONCLUSION

The addition of actuator saturation can degrade the transient performance of the system. The other extreme, actuator resolution limitations, can result in chatter, low fuel efficiency and a reduction in the achievable precision. In this paper, the resolution of the thruster is considered in the control problem of the formation flying system. It has been shown that when the thruster resolution is considered, chatter is introduced into the system and the performance of the system is degraded. Two methods were investigated to mitigate this problem. The first was an application of a pre-filter to smooth the command sent to the actuators. The pre-filter is used to compensate the discontinuity effects due to the minimum thrust level.

Based on the fuel consumption consideration, the pre-filter 1 is the preferred one. If the chattering and control precision are considered more, the pre-filter 2 case is preferred

Based on chattering and control precision results, pre-filter 1 is the preferred one. For this approach, three different prefilter designs were considered. The second approach was to modify the BLC; three modifications were also considered. The simulations, which were based on GA, illustrated the convergence of the three BLC schemes and that showed BLC1 has the best performance when considering the cost, fuel consumption, control precision and chattering.

There are currently efforts in this endeavor; for example, the colloidal thruster being developed by Busek can provide very small force, on the order of 1 micro-N. However, while colloidal thrusters may be able to achieve the types of actuator resolutions needed, they may not be able to deliver the levels of maximum thrust needed. Currently, the maximum force from these types of thrusters are on the order of 25 micro-N which may be too small to satisfy the mission requirements. Further study is needed to define the trades between actuator precision and mission accuracy.

REFERENCE

1. K. David Young, Vadim I. Utkin, Umit Ozguner, "A Control Engineer's Guide to Sliding Mode Control,' 1996 IEEE Workshop on Variable Structure Systems
2. Yunjun Xu, Norman Fitz-Coy, "Generalized Relative Dynamics and Control in Formation Flying System," 26th annual AAS Guidance and Control Conference, Breckenridge, Colorado, February 5 - 9, 2003
3. Yunjun Xu, Norman Fitz-Coy, and Paul Mason, "Genetic Algorithm based sliding mode control in the leader/follower satellites pair maintenance," 2003 AAS/AIAA Astrodynamics Specialist Conference, Big Sky, Montana, August, 2003
4. Yunjun Xu, Norman Fitz-Coy, and Paul Mason, "Coupled Orientation and Orbit Maintenance in Formation Flight Via Sliding mode control," J. of British Interplanetary Society, In review by GSFC
5. Gary J. Balas, and Andrew K. Packard, "Design of Robust, Time-Varying Controllers for Missile Autopilots," 1st IEEE Conference on Control Applications, Dayton, OH, Sept. 1992, pp. 13-16
6. R. Lind, G. Balas, and A. Packard, "Evaluating D-K iteration for Control Design," Proceedings of the American Control Conference, Baltimore, MD, June 1994, pp 2792-2797
7. R.T. Reichert, "Robust Autopilot Design Using μ-Synthesis," Proceedings of the American Control Conference, San Diego, CA, December 1990, pp. 2368-2373
8. G. P. Chen, O. P. Malik, and G. S. Hope, "Control Limits Consideration in Discrete Control System Design," IEE Proceedings-D, Vol. 140, No. 6, November 1993, pp. 413-422
9. J. E. Slotine and W. Li, *Applied Nonlinear Control*, Prentice Hall, Englewood Cliffs, New Jersey 1991
10. J. R. Carpenter, J. A. Leitner, R. D. Burns, and D. C. Folta, "Benchmark problems for spacecraft formation flying missions," AIAA Guidance Navigation and Control Conference, Austin, TX, August 2003